

UDC 539.3

EXPERIMENTAL STUDY OF PSEUDOELASTIC NITI ALLOY UNDER CYCLIC LOADING

Volodymyr Iasnii, Petro Yasniy

Ternopil Ivan Puluj National Technical University, Ternopil, Ukraine

Abstract. The phase transformation temperatures of pseudoelastic NiTi alloy were defined by differential scanning calorimetry. The effect of the stress range on the functional properties of the NiTi alloy under uniaxial tension in ice water at a temperature of 0 °C was studied. The cylindrical specimens with 4 mm in diameter and a gage length of 12.5 mm were tested under static and cyclic loading with the frequency of 0.5 Hz. All cyclic tests were performed under the crosshead displacement-controlled condition on the STM100 machine. At the temperature above A_f , the effect of the cyclic loading on the maximum stress, in general, could be characterized by several stages: strengthening, softening, stabilization and rapid decrease of the maximum stress, which is caused by the initiation and macrocrack growth. The increase of maximal stress in the first cycle from 509 MPa to 605 MPa increases the strain range.

Keywords: NiTi alloy, pseudoelasticity, differential scanning calorimetry, functional properties, maximal; stresses, strain range.

Received 09.01.2019

1. INTRODUCTION

Shape memory alloys (SMA) belong to functional materials characterized by the shape memory effect and pseudoelasticity. Their application depends on the temperature of phase transformations, mechanical and functional properties, the type of load (static, cyclic and thermomechanical).

Due to the high ability to dissipate energy, the SMA with the effect of pseudoelasticity is increasingly used in parts of machines, implants [1], damping devices [2-4], and other structural elements [5]. Since they are subjected to intense cyclic loadings during operation, it is important to ensure their reliability and durability for low-cycle fatigue.

Therefore, in order to construct the structural elements and devices made of SMA, it is necessary to study the regularities of changing stress and strain-based parameters, which characterize functional properties.

It is known that with the increase of load cycle numbers, the SMA functional properties (hyperelasticity effect), which can be characterized by the strain range and residual strain [6], get worse. The effect of maximum stress, mean stress and stress amplitude on SMA cyclic behaviour is investigated. It is determined that the maximum strain depends, in general, on the stress level and load type.

Particularly, residual and transformation hardening increase with the growth of loading cycles number and strain rates from $3,3 \cdot 10^{-4} \text{ s}^{-1}$ до $3,3 \cdot 10^{-2} \text{ s}^{-1}$ in super-elastic NiTi SMA micro-tube (50.32 % Ni) specimens in 2.5 mm in diameter during strain-controlled testing [7].

The residual strain growth was also observed for low-cycle fatigue of the wire made of NiTi alloy under uniaxial tension [8].

The residual deformation is usually considered to be related with some oriented martensite, which is not transformed back into austenite during the reverse phase [9]. Repeated changes in the direct and reciprocal phases create some defects in the material [10], resulting in localized internal stresses [11], allowing SMA to detect a two-way shape-memory effect.

The influence of the stress range on functional properties of Ni_{55,8}Ti_{44,2} alloy at a temperature higher than the temperature of austenitic transformation completion is investigated experimentally.

2. EXPERIMENTAL METHODS

The effect of cyclic loading on Ni_{55,8}Ti_{44,2} alloy functional properties in the form of 8 mm diameter rod supplied by Wuxi Xin Xin glai Steel Trade Co., LTD (China) was investigated. The chemical composition of the alloy, stated in the certificate: 55,78% Ni; 0,005% Co; 0,005% Cu; 0,005% Cr; 0,012% Fe; 0,005% Nb; 0,032% C; 0,001% H; 0,04% O; 0,001% N; 44,12% Ti.

Characteristics of thermal transitions during SMA phase transformations were investigated using Differential Scanning Calorimetry (DSC) [12] by means of DSC Q1000. The cylindrical specimen 1 mm in diameter with one flat side and 17,2 mg weight cut from Ø 8 mm rod were placed on a crucible plate made of Al₂O₃. Gas flow velocity was 30 ml/min. The specimen was heated and cooled from -150 to +120°C in nitrogen atmosphere N₂ and helium He₂ at 10°C/min rate. To increase the reliability of the obtained results, each of the heating and cooling cycles was repeated three times.

Mechanical properties and cyclic loading influence on the functional properties of NiTi alloy were investigated at 0°C temperature under the uniaxial tension of cylindrical specimens 4 mm diameter and 12.5 mm operating area length cut from Ø 8 mm rod (Fig.1a). The specimens were tested on the servohydraulic machine STM-100 [13] with automated control and data acquisition system under maximum uniform stem shifting with 0.5 Hz load frequency and sinusoidal cycle shape. Asymmetry coefficient of the load cycle $r = s_{\min} / s_{\max} = 0$ (here s_{\min}, s_{\max} is the lowest and largest value of the stem shifting). During the tests for the first and the following load cycles at $s_{\min} = 0$, the strains in the specimens were not observed.

The current values of force, stem shifting, and the longitudinal deformation of the specimen operating area with a 12 mm measuring base were recorded during the test. Longitudinal deformation was measured by Bi-06-308 extensometer produced by BISS; maximum error did not exceed 0.1%. The stem shifting was determined by an inductive Bi-02-313 sensor with an error of not more than 0.1%. The tests were carried out in the chamber filled with ice and ice water (Fig.1b). This provided the steady temperature of 0°C measured by a chromel-alumel thermocouple mounted on the specimen with an error not more than 0,5°C.

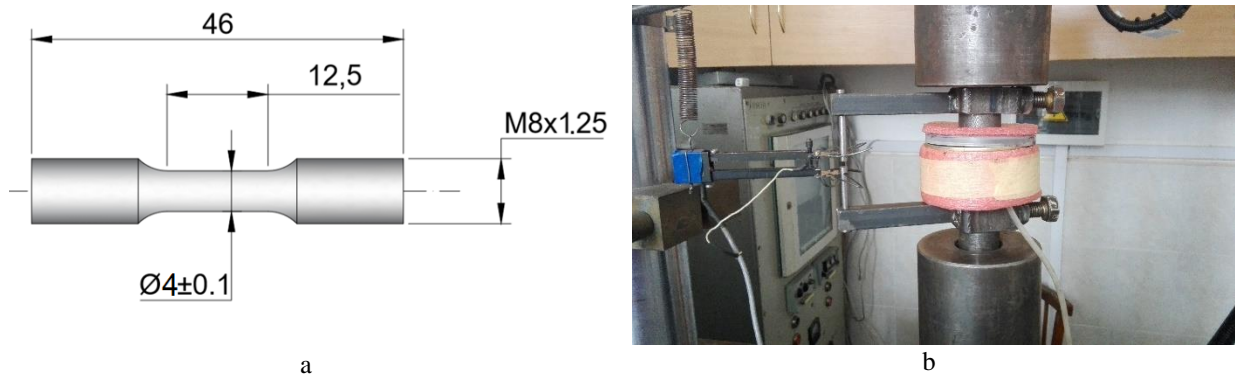


Figure 1. Specimen for fatigue tests – a; chamber with ice water for cooling the specimen installed with extensometer on the STM-100 machine – b.

3. RESULTS AND DISCUSSION

DSC analysis in coordinates heat-temperature (F - T): the curves demonstrate the martensitic-austenitic (Fig. 2a) and austenitic-martensitic (Fig. 2b) phase transformations occurring in SMA during the heating and cooling cycles relatively. A comparison of the phase transition temperatures confirms the reversible nature of the change in the crystallographic structure of the investigated material. While heating the specimen, the phase transition takes place in the temperature range between $-60,5^{\circ}\text{C}$ and $-38,7^{\circ}\text{C}$ (extrapolation of the average value), and the transition temperature is $-45,7^{\circ}\text{C}$. The reverse phase transition during cooling is between $-95,9^{\circ}\text{C}$ and $-69,4^{\circ}\text{C}$, and the heat flow reaches its maximum at $-81,4^{\circ}\text{C}$.

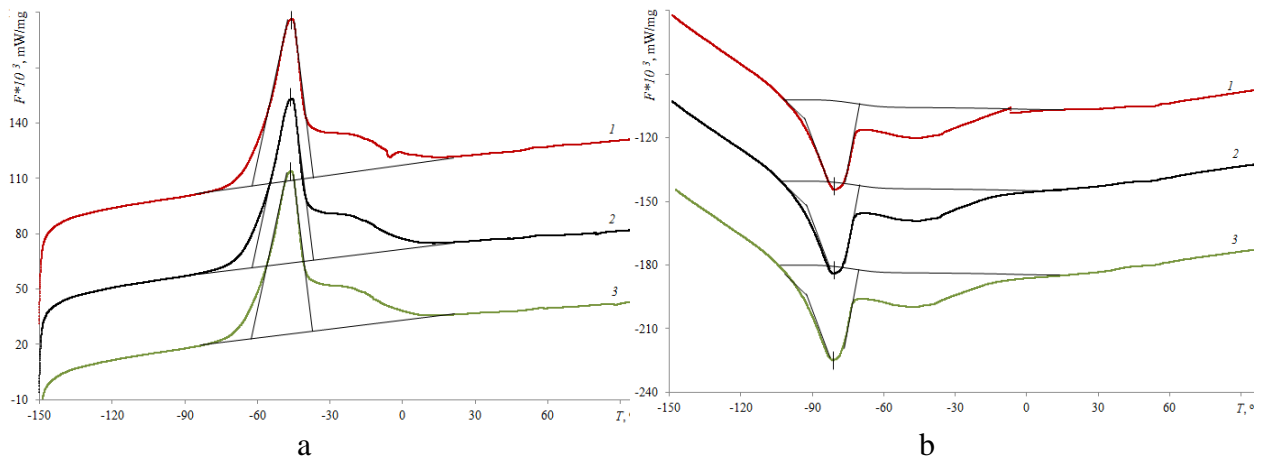


Figure 2. DSC analysis during first (1), second (2) and third (3) heating (a) and cooling (b) mode.

The enthalpy change caused by phase transitions was $12,43 \text{ J/g}$ during heating and $11,07 \text{ J/g}$ for cooling (Fig. 3).

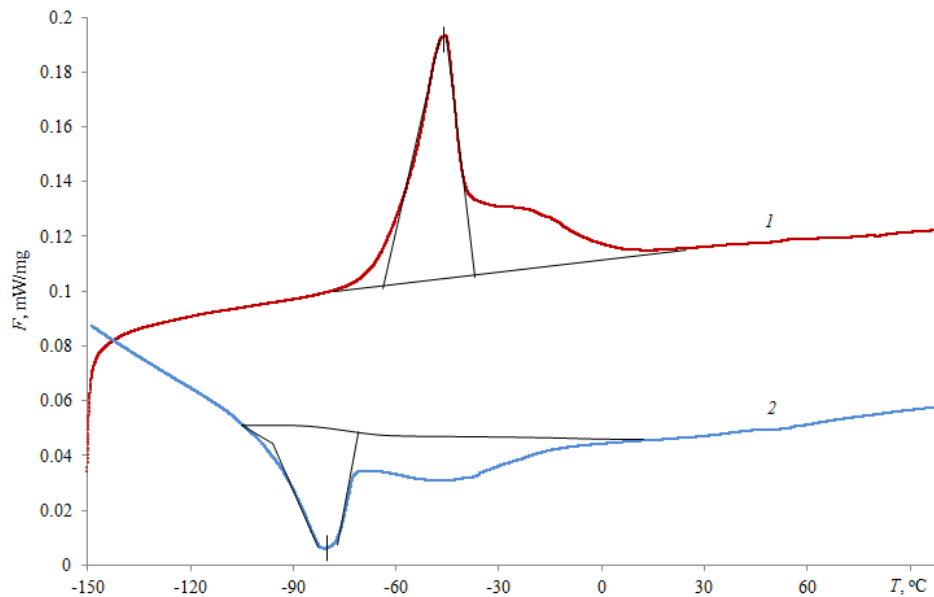


Figure 3. Enthalpy change during phase transformation of SMA in heating (1) and cooling (2) mode.

Summarized results of the phase transformation temperatures of the investigated SMA are given in Table 1. Here M_s , M_f , A_s , A_f are the start and end temperatures of the martensitic and austenitic phase, respectively. It should be noted that the temperature of the phase transformations in the wire material has a slight dispersion between separate heating (cooling)

cycles. Thus, the maximum deviation from the average temperature value of A_f austenitic transformation completion is $0,3^{\circ}\text{C}$ and for M_f is $0,7^{\circ}\text{C}$.

Table 1. Temperature of phase transformations in NiTi alloy.

Heating / cooling	M_s	M_f	A_s	A_f
	°C			
1-e	-68,7	-95,5	-60,3	-38,5
2-e	-69,6	-95,9	-60,5	-38,5
3-e	-70,0	-96,2	-60,6	-39,0
Averaged value	-69,4	-95,9	-60,5	-38,7

Characteristics of the mechanical properties of the alloy were determined according to standard [14] at 0°C temperature, which was higher than the temperature of the martensitic-austenitic transformation completion $A_f = -38,7^{\circ}\text{C}$ (Table 1).

The stretch diagram (Fig. 4) consists of three sections: I - elastic behaviour (austenitic phase); II - pseudoelastic (austenitic-martensitic phase), where the properties of hyperelasticity are observed; III - elastoplastic deformation (martensitic phase), which results in the specimen fracture.

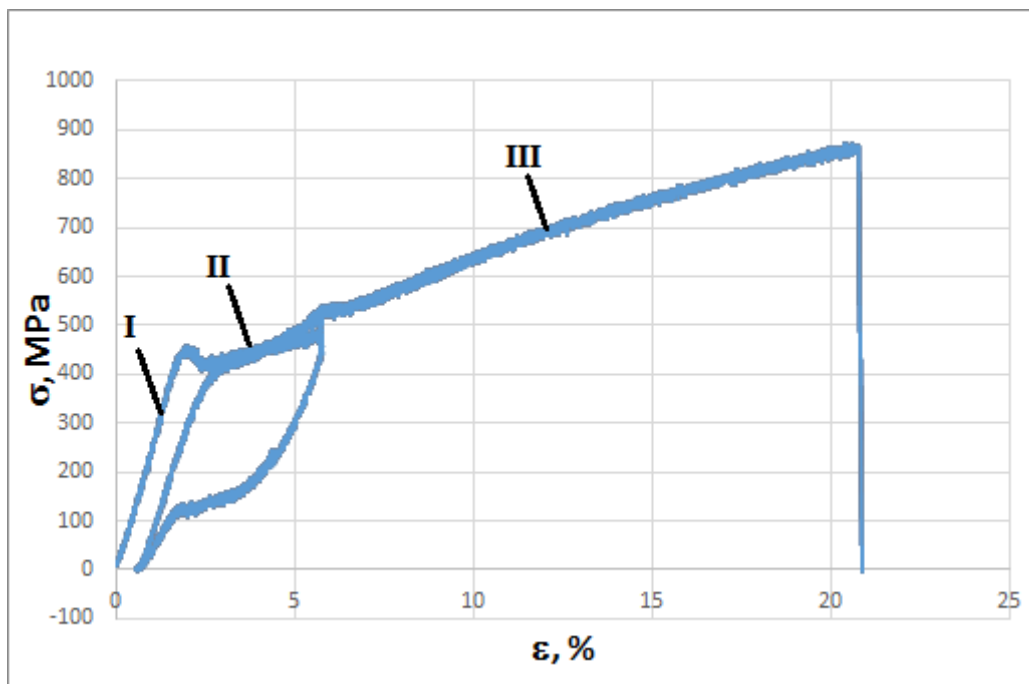


Figure 4. Stress-strain diagrams of SMA at 0°C : I – austenitic phase; II – austenite-martensitic; III – martensitic.

Characteristics of the alloy mechanical properties are given in Table. 2

Table 2. Mechanical properties of NiTi alloy at 0°C .

Yield Strength, $\sigma_{0,2}$	Ultimate Tensile Strength, σ_{UTS}	Young's Modulus, GPa	
MPa		I section	II section

447	869	25.3	16.9
-----	-----	------	------

Dependences of the maximum stress σ_{\max} and strain range of SMA on the number of load cycles for different starting values $\sigma_{\max} = \sigma_1$ are shown in Fig. 5 a,b. For all values of the initial maximum stress, during the first load cycles, the growth of in σ_{\max} value (material strengthening) is observed, then the weakening and stabilization, followed by the decrease section in the maximum stress caused by the macrocrack initiation and its growth. An exception is only the specimen with the initial maximum stress $\sigma_1 = 748$ MPa, which continuously decreased during operation time [15].

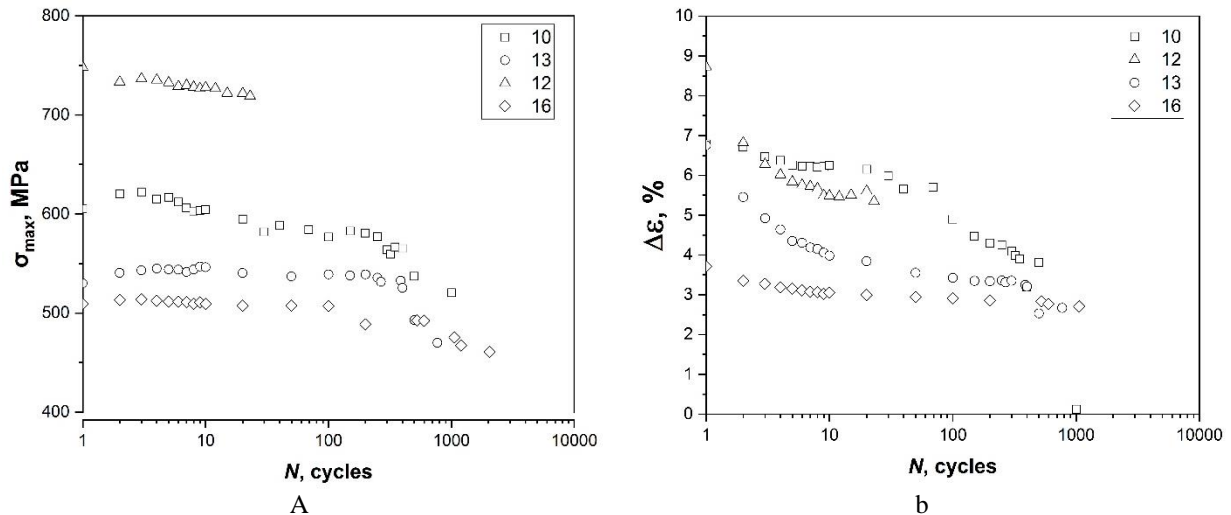


Figure 5. Dependences of the maximum stress - a and strain range - b on the number of loading cycles of SMA for $\sigma_1 = 509$ MPa (16) MPa, 530 MPa (13), 605 MPa (10), 748 MPa (12). The number of specimen are indicated in brackets.

Functional properties of the shape memory alloy (hyperelasticity) can be characterized particularly by the magnitude of strain range per cycle.

For all values of the initial maximum stress, during the first ten load cycles, there is a rapid decrease in the strain range followed by the stabilization area of the strain range or its less intensive decrease followed by a recession area resulting in the specimen fracture (Fig. 5b). With the increase of the maximum stress in the first load cycle from 509 MPa to 605 MPa, the strain range value increases (Fig. 5b).

In general, the strain range depends on the initial maximum stress, with the increase of which the strain range increases.

4. CONCLUSIONS

1. The temperature of forward and reverse phase transitions of pseudoelastic NiTi alloy is determined by differential scanning calorimetry technique.
2. The influence of stress range on the strain regularities and functional properties of pseudoelastic NiTi alloy in ice water at 0°C is studied, and appropriate methodology is developed.
3. At a temperature higher than the temperature of the martensitic-austenitic transformation finish under controlled crosshead displacement, the influence of the cyclic loading on the maximum stress can be characterized in general by areas of strengthening, weakening, stabilization and rapid decrease of the maximum stress caused by fatigue macrocrack initiation and extension.

4. The rapid decrease of the strain range observed during the first ten loading cycles, without regard to the initial value of the maximum stress, followed by the stabilization area, which changes into the area of continuous strain range reducing, ending with fracture of the specimen.

Reference

1. Auricchio F., Boatti E., Conti M. SMA Biomedical Applications // Shape Mem. Alloy Eng. Butterworth-Heinemann, 2015. P. 307–341.
2. Yasniy P. et al. Calculation of constructive parameters of SMA damper // Sci. J. TNTU. 2017. Vol. 88, № 4. P. 7–15.
3. Torra V. et al. The SMA: An Effective Damper in Civil Engineering that Smoothes Oscillations // Mater. Sci. Forum. 2012. Vol. 706–709, № July 2015. P. 2020–2025.
4. Isalgue A. et al. SMA for Dampers in Civil Engineering // Mater. Trans. 2006. Vol. 47, № 3. P. 682–690.
5. Menna C., Auricchio F., Asprone D. Applications of shape memory alloys in structural engineering // Shape Memory Alloy Engineering. 2015. 369–403 p.
6. Kang G. et al. Whole-life transformation ratchetting and fatigue of super-elastic NiTi Alloy under uniaxial stress-controlled cyclic loading // Mater. Sci. Eng. A. Elsevier, 2012. Vol. 535. P. 228–234.
7. Kan Q. et al. Experimental observations on rate-dependent cyclic deformation of super-elastic NiTi shape memory alloy // Mech. Mater. Elsevier, 2016. Vol. 97. P. 48–58.
8. Moumni Z., Zaki W., Maitournam H. Cyclic Behavior and Energy Approach to the Fatigue of Shape Memory Alloys // J. Mech. Mater. Struct. 2009. Vol. 4, № 2. P. 395–411.
9. Auricchio F., Marfia S., Sacco E. Modelling of SMA materials: training and two way memory effect. // Comput. Struct. 2003. Vol. 81. P. 2301–2317.
10. Abeyaratne R., Kim S.-J. Cyclic effects in shape-memory alloys: a one-dimensional continuum model // Int. J. Solids Struct. Pergamon, 1997. Vol. 34, № 25. P. 3273–3289.
11. Tanaka K. et al. Phenomenological analysis on subloops and cyclic behavior in shape memory alloys under mechanical and/or thermal loads // Mech. Mater. Elsevier, 1995. Vol. 19, № 4. P. 281–292.
12. Iasnii V., Junga R. Phase Transformations and Mechanical Properties of the Nitinol Alloy with Shape Memory // Mater. Sci. 2018. Vol. 54, № 3. P. 406–411.
13. Yasniy P. V. et al. Microcrack initiation and growth in heat-resistant 15Kh2MFA steel under cyclic deformation // Fatigue Fract. Eng. Mater. Struct. Blackwell Science Ltd, 2005. Vol. 28, № 4. P. 391–397.
14. ASTM F2516-14. Standard Test Method for Tension Testing of Nickel-Titanium Superelastic Materials. Book of Standards Volume: 13.02. 2014.
15. Iasnii V., Budz V., Antonchenko V., Holubovskiy M. Modelling of the functional properties of the SMA-based damper device // Procedia Structural Integrity, 2024. 59, P. 299–306.

УДК 539.3

ДОСЛІДЖЕННЯ НАДПРУЖНОЇ ПОВЕДІНКИ NITИ СПЛАВУ ЗА ЦИКЛІЧНОГО НАВАНТАЖЕННЯ

Володимир Ясній, Петро Ясній

Тернопільський національний технічний університет імені Івана
Пулюя, Україна

Резюме. Методом диференціальної сканувальної калориметрії досліджено температуру прямих і зворотних фазових переходів нікельтитанового сплаву $Ni_{55,8}Ti_{44,2}$. Зіставлення температур фазових переходів підтверджує зворотний характер зміни кристалографічної структури досліджуваного матеріалу. Під час нагрівання зразка фазовий перехід відбувається в діапазоні температур між $-60,5^{\circ}\text{C}$ та $-38,7^{\circ}\text{C}$, а температура переходу становить $-45,7^{\circ}\text{C}$. Таким чином температури початку і завершення аустенітної фази склали відповідно $A_s = -60,5^{\circ}\text{C}$ і $A_f = -38,7^{\circ}\text{C}$. Розроблено методуку і досліджено вплив розмаху напруження на закономірності деформування одновісним розтягом і функціональні властивості нікельтитанового сплаву за температури 0°C в середовищі талого льоду. Характеристики механічних властивостей і вплив циклічного навантаження на функціональні властивості сплаву досліджували за одновісного розтягу циліндричних зразків діаметром 4 мм і довжиною робочої ділянки 12,5 мм, які були вирізані з прутка $\varnothing 8$ мм. Частота навантаження за

синусоїдальної форми циклу складала 0,5 Гц. При температурі вище температури закінчення мартенситно - аустенітного перетворення СПФ, в умовах контрольованого переміщення затискачів вплив циклічного навантаження на максимальне напруження загалом можна охарактеризувати ділянками зміцнення, знеміцнення, стабілізації і стрімкого падіння максимального напруження, яке спричинене появою і поширенням макротріщини. Для усіх значень початкового максимального напруження, упродовж перших десяти циклів навантаження спостерігається стрімке зменшення розмаху деформації, потім слідує ділянка стабілізації розмаху деформації, або менш інтенсивного її зменшення, після якої слідує ділянка спаду, яка завершується руйнуванням зразка. Із збільшенням максимального напруження у першому циклі навантаження від 509 МПа до 605 МПа збільшується значення розмаху деформації.

Ключові слова: NiTi сплав, псевдопружність, диференціальна сканувальна калориметрія, функціональні властивості, максимальні напруження, розмах деформації.

Отримано 09.01.2019